

# Asymmetries in quasi-elastic ${}^3\vec{H}e(\vec{e}, e')$ (First attempt)

Miha Mihovilovic, Simon Sirca

September 21, 2009

## Abstract

In this document I will briefly describe my first attempt to determine the transverse asymmetry  $A_{T'}$  in  ${}^3\vec{H}e(\vec{e}, e')$  quasi elastic scattering. This asymmetry is sensitive to the neutron magnetic form factor  $G_M^n$ . In my analysis I will use  $Q^2 = 0.3(\text{GeV}/c)^2$  data, measured during the E05-102 experiment in Hall A at JLab. I will compare my results with the results from the experiment E95-001, where they measured  $G_M^n$  with very high precision.

## 1 Introduction

The electromagnetic form factors represent a very interesting topic in nuclear physics, because they contain the information about the distribution of charge and magnetization within nucleons. Knowing the form factors allows us to test various nucleon models based on quantum chromodynamics. This advances our knowledge of nucleon structure and provides a basis for the understanding of strongly interacting matter in terms of quark and gluon degrees of freedom.

We can not measure the neutron electromagnetic form factors directly, but need to determine (extract) them from the measured nuclear cross-sections. For unpolarized elastic electron scattering off a nucleon, the cross section can be written as [1]

$$\left(\frac{d\sigma}{d\Omega}\right) = \left(\frac{d\sigma}{d\Omega}\right)_{Mott} \cdot \left[ \frac{G_E^2(Q^2) + \tau G_M^2(Q^2)}{1 + \tau} + 2\tau G_M^2(Q^2) \tan^2 \frac{\theta}{2} \right]. \quad (1)$$

The Mott cross-section describes the elastic scattering off a point-like particle,  $\theta$  is the scattering angle and  $\tau = \frac{Q^2}{4M^2c^2}$ . Functions  $G_E(Q^2)$  and  $G_M(Q^2)$  are the electric and magnetic form factors, both of which depend upon  $Q^2$ . The measured  $Q^2$ -dependence of the form factors gives us information about the radial charge distributions and magnetic moments.

For the proton, (1) can be measured and applied directly. In order to determine proton form factors  $G_E^p$  and  $G_M^p$  we can observe electron scattering off the hydrogen target, which is a pure proton target. On the other hand, there are no free neutron targets. Consequently the neutron form factors  $G_E^n$  and  $G_M^n$  can not be measured directly as in (1) and are thus known with much poorer precision. In last couple of years a lot of effort has been put into a more precise determination of the neutron form factors.

A very nice approach to the precision measurement [2] of  $G_M^n$  is through the inclusive quasielastic reaction  ${}^3\vec{H}e(\vec{e}, e')$ . A polarized  ${}^3He$  target is very useful for studying the neutron structure, because its ground state is dominated by a spatially symmetric  $S$  wave in which proton spins cancel and the spin of the  ${}^3He$  nucleus is carried by the unpaired neutron (see figure 1).

In the case of polarized beam and polarized target, the cross-section for the  ${}^3\vec{H}e(\vec{e}, e')$  reaction has the general form

$$\frac{d\sigma(h, \vec{S})}{d\Omega_e dE_e} = \frac{d\sigma_0}{d\Omega_e dE_e} \left[ 1 + \vec{S} \cdot \vec{A}^0 + h(A_e + \vec{S} \cdot \vec{A}) \right], \quad (2)$$

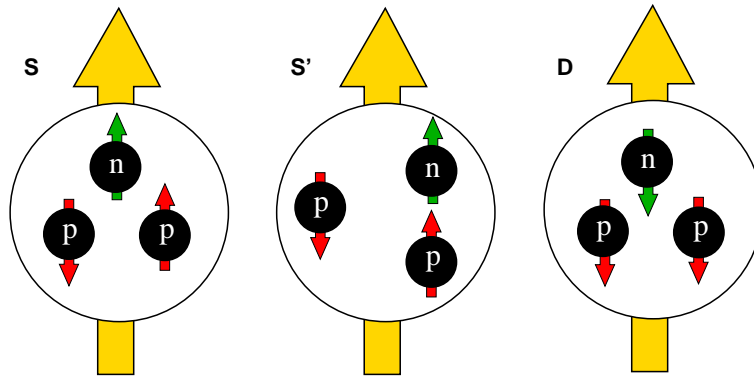


Figure 1: Three ground state configuration of the  ${}^3\text{He}$ .

where  $\sigma_0$  is the unpolarized cross-section,  $\vec{S}$  is the spin of the target and  $h$  is the helicity of the electrons. The  $\vec{A}^0$  and  $A_e$  indicate the asymmetries induced by the polarization of only the target or only the beam, while  $\vec{A}$  is the asymmetry when both the beam and the target are polarized [3]. The target quantization axis is chosen to be along the direction of momentum transfer. We will focus on the asymmetry  $\vec{A}$  of which only two components  $A_{x,z}$  are non-zero in coplanar geometry with the spin aligned in the scattering plane:

$$A_{x,z} = \frac{[d\sigma_{++} + d\sigma_{--}] - [d\sigma_{+-} + d\sigma_{-+}]}{[d\sigma_{++} + d\sigma_{--}] + [d\sigma_{+-} + d\sigma_{-+}]}, \text{ where } \begin{cases} A_x : (\vec{S}_x \perp \vec{q}) \\ A_z : (\vec{S}_x \parallel \vec{q}) \end{cases} \quad (3)$$

The  $(\pm, \pm)$  signs represent the beam helicities and the projections of the target spin along the quantization axis (x for  $A_x$  and z for  $A_z$ ). Asymmetries  $A_x$  and  $A_z$  must be measured separately since they require different spin orientations. Following this four-fold spin sequence, possible systematic uncertainties and contributions from  $\vec{A}^0$  and  $A_e$  can be greatly suppressed. This is the beautiful thing about this type of measurement.

From the theory it follows that the inclusive transverse asymmetry  $A_{t'} = A_x$  in the vicinity of the  ${}^3\text{He}$  quasi-elastic peak is most sensitive to the neutron magnetic form factor. In the first order plane-wave impulse approximation (PWIA) the transverse asymmetry  $A_{t'}$  can be written as [2]

$$A_{t'} \propto \frac{(G_M^n)^2}{a + b(G_M^n)^2}, \quad (4)$$

where at low  $Q^2$  the parameter  $a$  is much larger than  $b(G_M^n)^2$ . Figure 2 shows the transverse asymmetries at different  $Q^2$  that were measured in the E95-001 experiment. From these results we then determine how neutron magnetic factor depends on the  $Q^2$ . The final results are shown in figure 3.

## 2 Transverse asymmetries from E05-102 data

In the experiment E05-102 we were measuring double-polarized asymmetries in following exclusive reaction channels  ${}^3\vec{H}e(\vec{e}, e'd)$ ,  ${}^3\vec{H}e(\vec{e}, e'p)$  and  ${}^3\vec{H}e(\vec{e}, e'n)$ . For the measurement of the neutron channel ( $e, e'n$ ) we were using the neutron detector (HAND) in coincidence with the Right High Resolution Spectrometer (HRS-R). For the ( $e, e'p$ ) and ( $e, e'd$ ) channels we were using the BigBite Spectrometer in coincidence with the Left High Resolution Spectrometer. The purpose of this measurement is to test the state-of-the-art Faddeev calculations of the three-body system [3] and to study the  $S'$ -state and  $D$ -state contributions to the  ${}^3\text{He}$  ground-state wave-function.

Once we are ready to extract the beam-target asymmetries  $A_x$  and  $A_z$ , we need to make sure that procedures, algorithms, cuts, etc. work properly, so that asymmetries and conclusions that we will draw from them will be real. One way is to compare the analyzed data with the theory. This is not easy due to the complexity of the theoretical results that we poses. By doing that we are also biased, because we will be correcting our potential mistakes until measurements and theory will agree. This is not right since we are searching for the

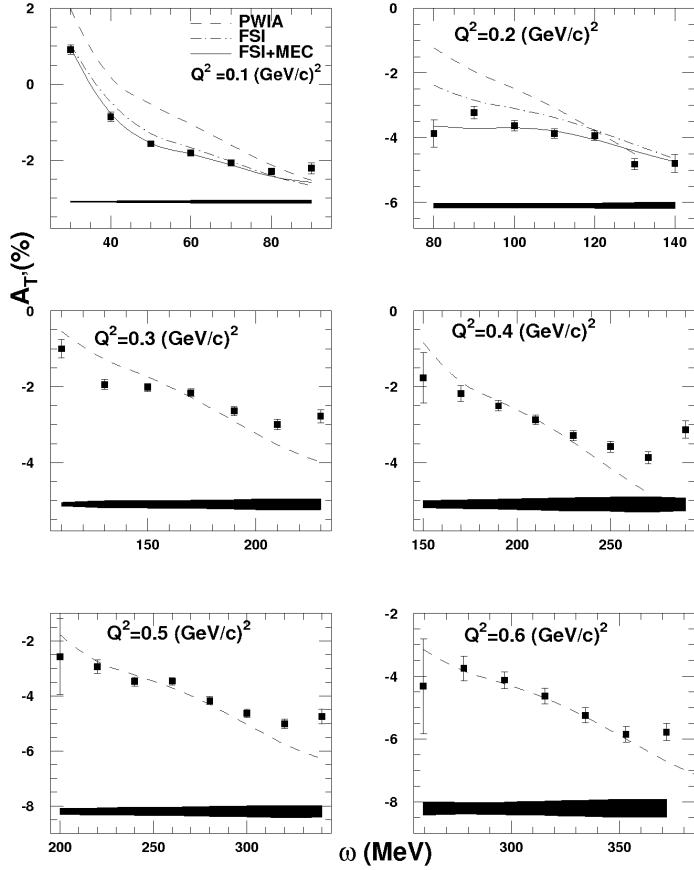


Figure 2: The transverse asymmetry  $A_{T'}$  in  $Q^2 = 0.1 - 0.6(\text{GeV}/c)^2$  measured during the E95-001 experiment [2]. The experiment was carried out in Hall A at the Thomas Jefferson National Accelerator Facility (JLab), using a longitudinally polarized continuous wave electron beam of  $10 \mu\text{A}$  current incident on a high-pressure polarized  $^3\text{He}$  gas target. The beam and target polarizations were approximately 70% and 30%, respectively. Six kinematic points were measured corresponding to  $Q^2 = 0.1$  to  $0.6(\text{GeV}/c)^2$  in steps of  $0.1(\text{GeV}/c)^2$ . An incident electron beam energy  $E_b = 0.778\text{GeV}$  was employed for the two lowest  $Q^2$  values of the experiment and the remaining points were completed at  $E_i = 1.727\text{GeV}$ . To maximize the sensitivity to  $A_{T'}$ , the target spin was oriented at  $62.5^\circ$  to the right of the incident electron momentum direction.

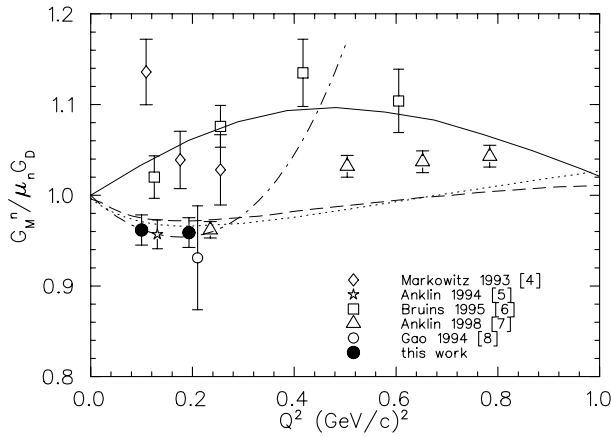


Figure 3: The neutron magnetic form factor  $G_M^n$  in units of the standard dipole form factor  $(1 + \frac{Q^2}{0.71})^{-2}$ , as a function of  $Q^2$ , along with previous measurements and theoretical models. Lines represent various theoretical models[2].

true physical asymmetries and not those that agree with the theoretical models. Therefore it would be better to check our analysis somehow differently.

It is better to compare our measurements with some other data. The idea is to use the same procedure, as we will use on the exclusive channels, on our inclusive data  $^3\text{He}(e, e')$ . From them we should be able to reconstruct the  $G_M^n$  asymmetries from the E95-001.



Figure 4: The figure shows open detector hut of the HRS-L spectrometer with the detector packages and electronics in it.

In this report I will describe my first attempt to determine the quasi-elastic asymmetries from our data. This is an initial step in our analysis and will represent a sanity check rather than being a serious analysis. There is a lot of work that needs to be done, like spectrometer and target calibration, before we will be able to determine accurate asymmetries.

Before we can proceed with the calculation of the asymmetries, we first need to determine and check some other, more basic quantities. We first need to know how the beam and target polarization was changing during the experiment and what was the target polarization orientation, the dilution factors, collected charge and dead time during each run. All these parameters affect our final results, and each of these elements requires a detailed analysis. In this report I will present the results of the first-pass analysis of each of these corrections.

## 2.1 Target Polarization and $\vec{B}$ orientation

In the experiment we were using a high-pressure polarized  $^3\text{He}$  target. The target system consists of a moving target ladder with various targets attached to it, a holding magnetic field system, heating system and a laser optics system. Beside the polarized  $^3\text{He}$  target we were also using a carbon 7-foil target for the optical calibration of the spectrometers and an unpolarized (reference) gas target. We were able to put various gases ( $^3\text{He}$ ,  $\text{D}_2$ ,  $\text{N}_2$ ,  $\text{H}_2$ ) at various pressures into this cell and used it for the determination of the dilution factors.

Our polarized  $^3\text{He}$  target is made of a 40cm long glass cell (see figure 5) filled with a high pressure 3He gas ( $7.93 \text{ amg}^1$ ) and a small amount of vapor of rubidium-potassium mixture. The target employs the so-called spin-exchange optical pumping technique.  $^3\text{He}$  is polarized in a two-step process. First, rubidium vapor is polarized by optical pumping with circularly polarized 795 nm laser light. Second, the polarization of the Rb atoms is transferred to the  $^3\text{He}$  nucleus in spin-exchange collisions, in which  $^3\text{He}$  nuclei are polarized via the hyperfine interaction. In addition, target also contains a small amount of nitrogen to increase the pumping efficiency.

Experiment required a flexible alignment of the target polarization vector parallel to (for  $A_z$  asymmetry) and perpendicular to (for  $A_x$  asymmetry) the direction of the momentum transfer  $\vec{q}$ . We are using three Helmholtz coils to rotate and hold the polarization in any chosen direction (see figure 6). Unfortunately, we can optically pump only in three directions : longitudinal, transverse and vertical. If we want a polarized target in an arbitrary direction we first have to polarize it in one of these three directions and then rotate it to the chosen direction. Unfortunately without constant pumping the polarization rapidly decreases and can be used for only a few hours. Afterwards, when the polarization would drop too much, we would have to rotate the target again to its original direction to restore the polarization. This takes approximately four to eight hours and in the meanwhile the

<sup>1</sup>An amagat is a practical unit of number density. Although it can be applied to any substance at any conditions, it is defined as the number of ideal gas molecules per unit volume at 1 atm [?].

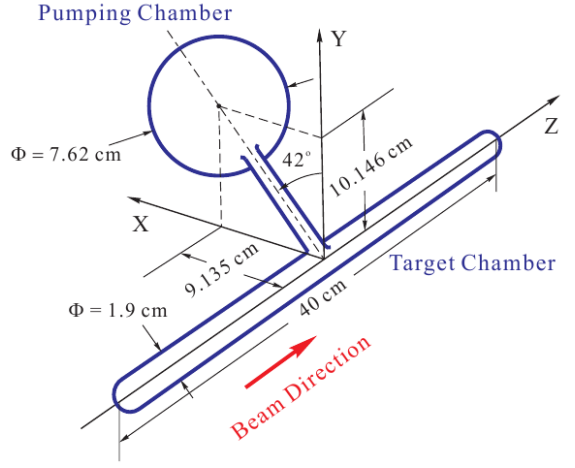


Figure 5: *Left:* Polarized  $^3\text{He}$  cell mounted on the target ladder inside the target enclosure. *Right:* Schematics of the target cell. It consist of two main parts: the oval main target cell, which is put into the beam line and where the reactions happen, and a spherical pumping chamber (positioned outside the beam line) where incident laser light hits the  $^3\text{He}$  gas and polarizes it.

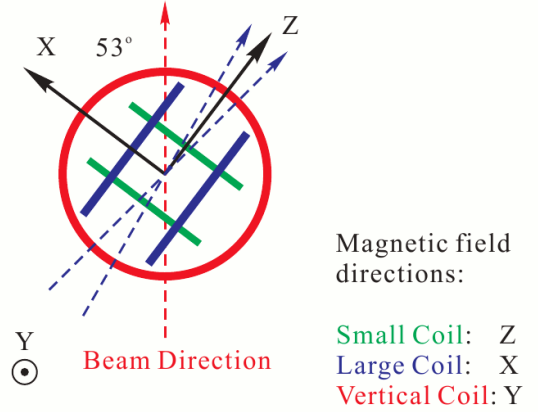
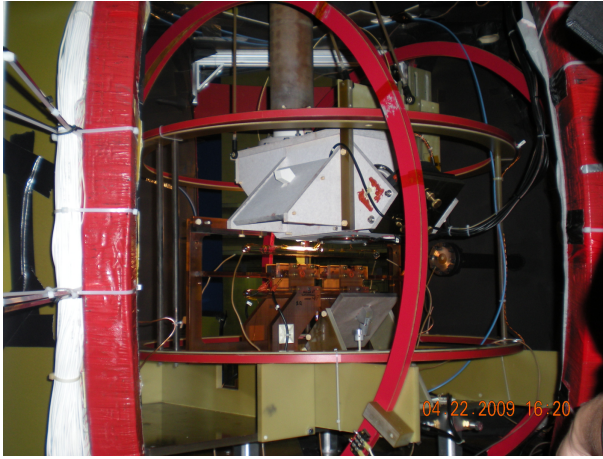


Figure 6: *Left:* Target enclosure with target ladder and three pairs of Helmholtz coils (red stripes). *Right:* Schematic representation of the Helmholtz coil orientation with respect to the beam direction.

polarized target can not be used with beam. Therefore we decided not to measure the asymmetries  $A_z$  and  $A_x$  directly, but to measure the asymmetries  $A_L$  (target spin oriented along the beam line) and  $A_T$  (target spin oriented perpendicular (to the right) of the beam direction) and post-festum determine the true asymmetries by using the rotations:

$$\begin{pmatrix} A_x \\ A_z \end{pmatrix} = \begin{pmatrix} \cos \theta_q & \sin \theta_q \\ -\sin \theta_q & \cos \theta_q \end{pmatrix} \begin{pmatrix} A_L \\ A_T \end{pmatrix}, \quad (5)$$

where  $\theta_q$  is the in-plane angle between the direction of the incident beam and the momentum transfer  $\vec{q}$ . Figure 7 shows how the currents in all three Helmholtz coils were changing during the experiment. This directly corresponds to the orientation of the field and the target spin. In the experiment E05-102 we were only interested in the two in-plane asymmetries and did not measure the asymmetry with the vertical orientation of the spin. Therefore the current in the vertical coil was always constant. We switched between the longitudinal and transversely polarization several times. In the longitudinal direction we were able to polarize only in the direction along the beam (Longitudinal +). Optical pumping in the opposite direction (Longitudinal -) was not possible

because of the limits of our optical system. In the transverse direction, however, we were able to polarize target in direction to the right of the beam (Transverse +) as well as in direction to the left of the beam (Transverse -).

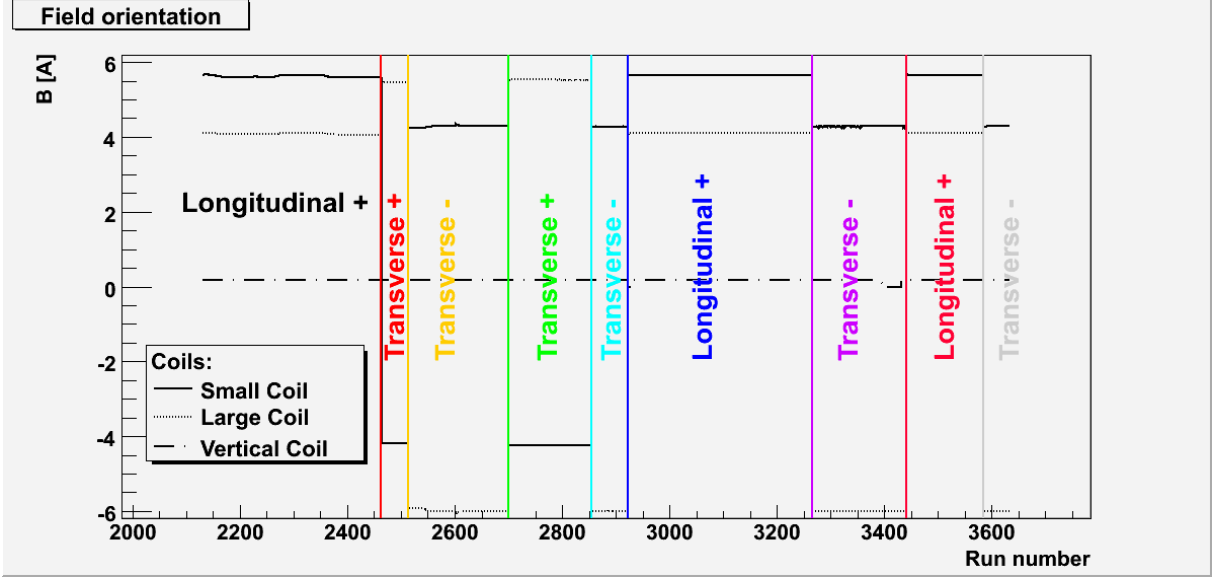


Figure 7: Currents in all three Helmholtz coils (and corresponding field orientations) during the experiment.

The target polarization  $P_t$  was monitored with a nuclear magnetic resonance (NMR) system. The response of the NMR system for  $^3\text{He}$  has been calibrated with the NMR measurements on water. The calibration was also independently verified by measurements of the frequency shifts in the lines of electron paramagnetic resonance (EPR) caused by polarized  $^3\text{He}$  nuclei. The water cell calibration test were made at the beginning of our experiment, while the EPR measurements on polarized  $^3\text{He}$  target were made approximately once a week. NMR polarization measurements were made every two to four hours (this means approximately after every eighth run), depending on the beam current, orientation of the target and a kind of measurements that were we performing at the moment. Plot 8 shows how target polarization changed during the experiment. The maximum polarization was approximately 66% and was reached for the longitudinally polarized target.

### 3 Target Cell Wall Subtraction

When estimating the asymmetries we need to consider many corrections that can affect our final result. A small but not negligible correction is the target-cell-window correction. Incident electrons scatter on the  $^3\text{He}$  atoms as well as on the atoms of the glass windows on the each side of the cell. The first thing that we can do is of course a cut around the glass windows, and consider only the interior of the cell. This way we get rid of the majority of the contamination with the glass. However, the tails of the window distribution can reach deep into the interior of the cell and that also needs to be considered. To determine this factor I took an empty cell (no gas in the reference cell) run and compared it with the production run. Since the collected charge and dead time can be different for each run I had to renormalize one of the runs so that I was then able to compare them. I decided to renormalize the empty-cell run in a way that positive- $TgY$  peaks (see figure 9), which correspond to the entrance window, have the same amplitude. I have argued this choice with the fact that the number of scattered electrons from this window does not depend on the content of the target behind the first window. For the exit-window this is of course not true. After the renormalization I subtracted the empty-cell run from the production run and the plot that I got should represent the pure helium target. Then I compared this plot with the full production run, using the ratio:

$$R(y_{tg}) = \frac{\int_{-y_{tg}}^{y_{tg}} H_{\text{Pure He}}(x) dx}{\int_{-y_{tg}}^{y_{tg}} H_{\text{Full He}}(x) dx} \quad (6)$$

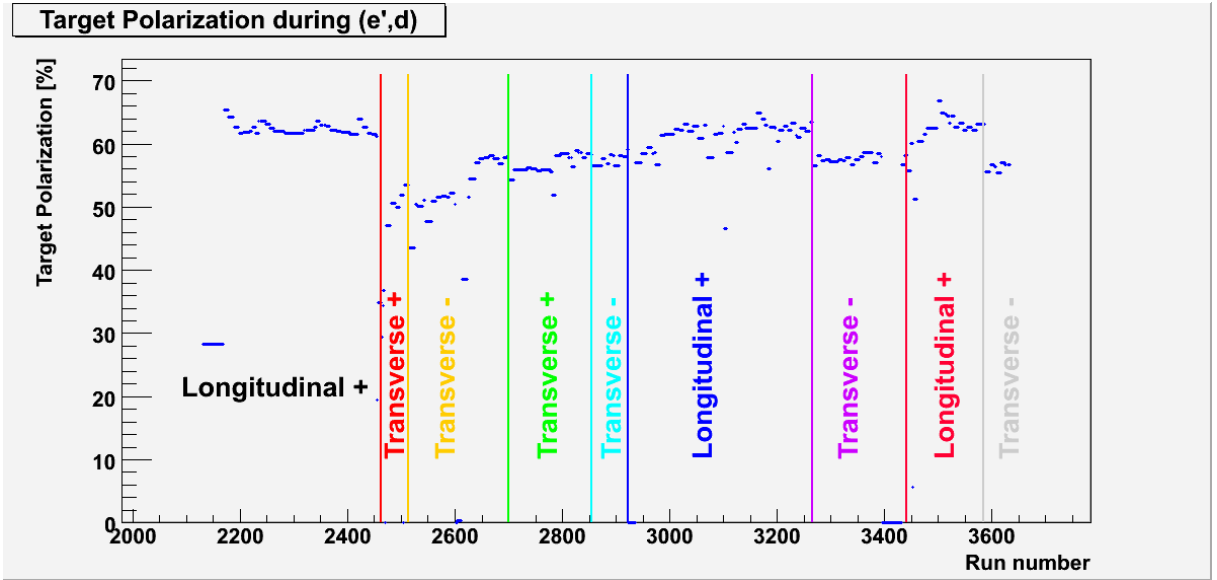


Figure 8: Target polarization during the experiment. Polarization values in this plot are direct readouts from the NMR polarization measurement system. These measurements were done approximately every eight runs.

where  $y_{tg}$  represents the distance from the target center and  $H(y_{tg})$  is the value of histogram at  $y_{tg}$ . From plot 10 we can see that within the majority of the target this correction is less than a percent. Therefore this correction will not affect our asymmetries very dramatically.

### 3.0.1 Polarized $^3He$ target vs. Reference Cell with $^3He$

The correction factor that will have the biggest effect on our asymmetries is the nitrogen dilution factor. There are two ways to determine this factor and in the end they both should agree. In the first one we could compare the helium production run with the calibration runs where we had nitrogen in the reference cell. By knowing the correct nitrogen pressure we can directly extract the nitrogen dilution factor, by performing the same ratios as we did for the target-window correction. Unfortunately at the moment we do not know the correct nitrogen pressure, because it still needs to be determined.

The other procedure is the exact opposite. Instead of nitrogen we put  $^3He$  in the reference cell and compare the yield with the polarized production run. Since we have only pure helium in the reference target we can determine the dilution factor by subtracting the two runs. Plots 11 and 12 show the results of this comparison. We can see that according to our measurement the dilution factor is approximately 10%. In our experiment we put approximately  $150psi$  of  $^3He$  in the reference cell, while at the moment we believe that the partial helium pressure in the production cell is  $109psi$ . This introduces additional factor of 1.4 to the determined dilution factor, assuming that  $^3He$  yield in the reference cell rises linearly with the pressure. In the end this gives a dilution factor of:  $f_{nitrogen} = 1 + 51\% = 1.51$ .

## 3.1 Beam properties

During the ( $e'd$ ) experiment we were using a longitudinally polarized continuous electron beam with an energy of 2.4 GeV (second pass beam). The beam helicity was flipped with frequency  $\approx 30$  Hz. When using a polarized beam we want to be sure that the beam charge asymmetry is as small as possible or at least smaller than the asymmetries that we are looking for, so that we do not introduce some false asymmetries to our measurements. For that purpose we were measuring the beam charge asymmetry during the whole experiment (see figure 13) and according to our measurements it was smaller than ( $500ppm$ ) throughout the whole experiment. In this experiment we took approximately one half of the runs with the beam half-wave plate in and another half with beam half-wave plate out. This plate is inserted in the injector in front of a laser that hits the photo-cathode from which initial polarized electrons are emitted before being accelerated. The position of this plate is independent of any settings in the experimental hall and is a good sanity check to see if our apparatus works properly. If

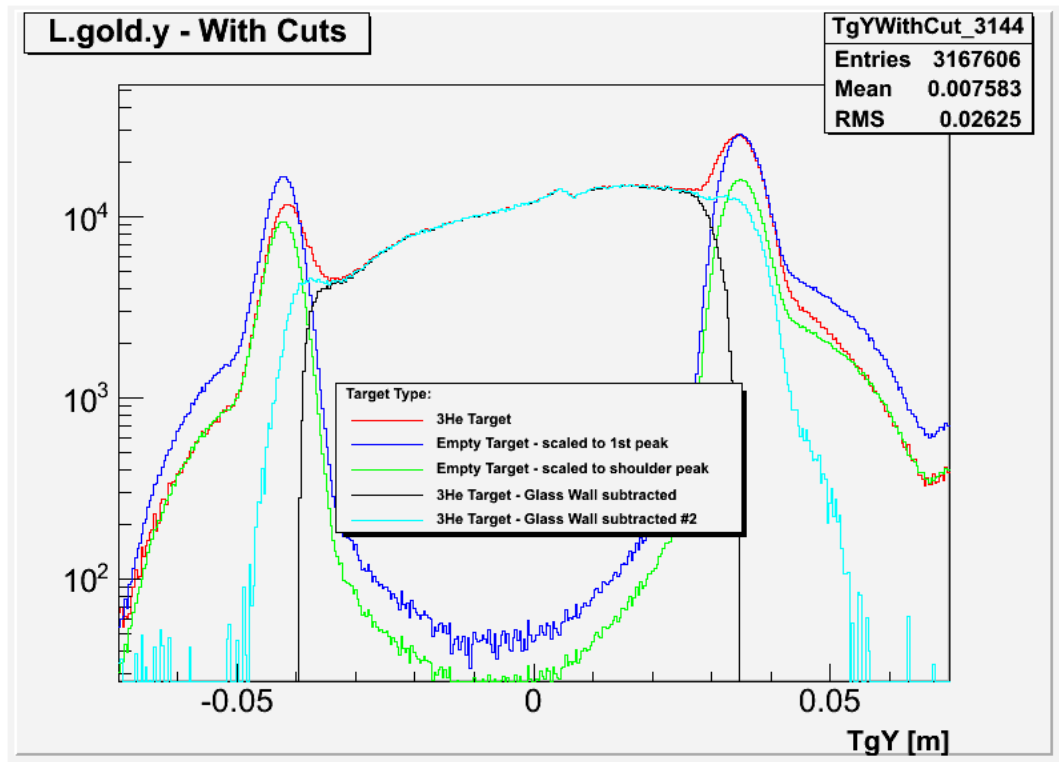


Figure 9: The red line represents the target  $y_{tg}$  coordinate for the production  ${}^3\text{He}$  run, the blue line represents the  $y_{tg}$  coordinate for the empty-cell run and the black line represents the difference between the two. In this case the empty cell run was normalized to the amplitude of the right peak. I have also tried another approach, where I normalized the empty-cell run to the slope at the beginning and at the end of the target (green line), but did not decide to use it. In that case the cyan line represents the pure helium yield.

there is no other change made to the experimental configuration when the position of the  $\lambda/2$ -plate is changed (in/out) all our physical asymmetries should flip. Plot 14 shows how the position of the  $\lambda/2$ -plate was changing during the experiment.

The polarization of the beam was measured independently with Møller and Compton polarimeters. During the experiment we did only three Møller measurements, because it takes approximately four hours to do such measurement (see figure 15). According to this measurements the beam polarization was approximately 88%. The Compton polarimeter was working through the whole experiment but we still do not have the polarization results from it due to the problems with polarimeter. Therefore at the moment we need to rely on the Møller measurements.

### 3.2 Analysis Results

Now that we have covered all the basics, we can proceed and finally try to calculate the asymmetries. Determination of the polarization is fairly simple, once everything is properly calibrated (database files contain correct parameters so that optics modules work correctly) and appropriate cuts are used. In this analysis I have used only the most basic cuts:

- $|y_{Tg}| \leq 0.025$  : With this cut I limit my analysis only to those events that come from the middle portion of the target cell, where I am certain that I will not have problems with the effects near the boundaries.
- `DL.eventtypebits&8 == 8` : In our experiment we were using different triggers each describing a particular type of events. We separate all the recorded events by the triggers that were accepted for that particular event. All the accepted triggers are recorded in the `DL.eventtypebits` variable. We set various prescale factors to our triggers and consequently all triggers are not recorded every time. If we are trying



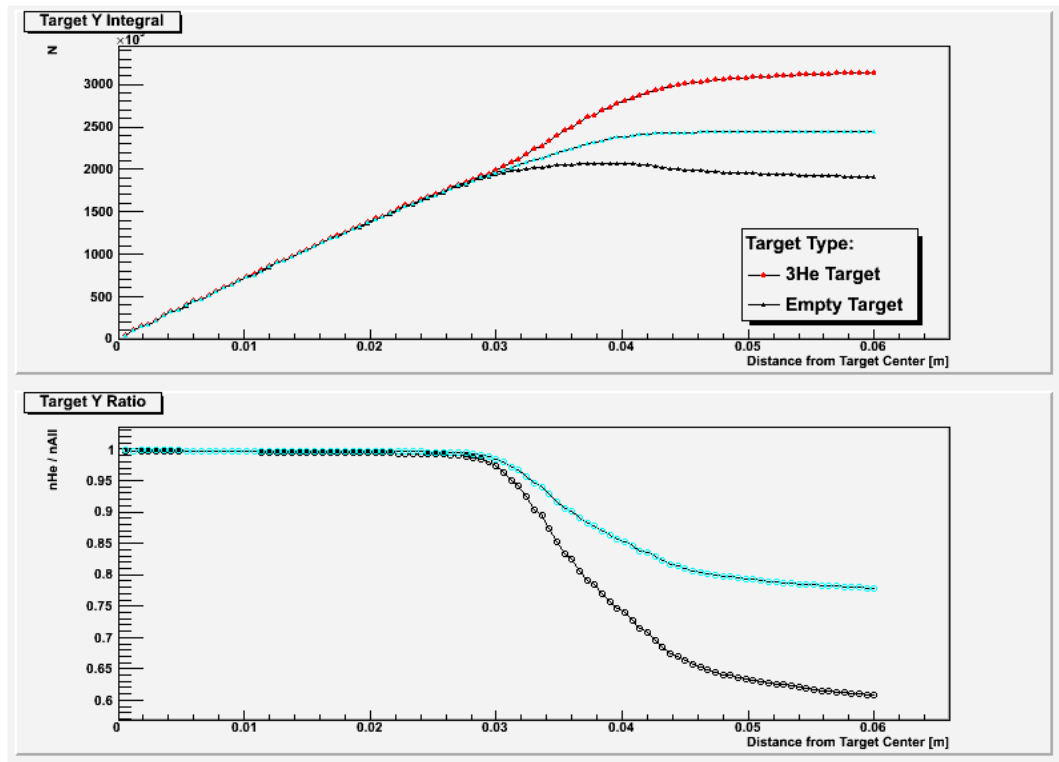


Figure 10: *Top*: The integral of the Target  $y_{tg}$  histogram as a function of the distance from the target center. Red line corresponds to the full  ${}^3\text{He}$  run while the black line represents the integral of the pure helium response. *Bottom*: The ratio between the pure helium yield ( ${}^3\text{He}^{Pol.}$  – Empty Cell) and a complete polarized target yield.

to determine the inclusive asymmetry from the  ${}^3\text{He}(e, e')$  reaction we are interested only in those events that were seen by the spectrometer, that was used for the detection of scattered electrons (HRS-L). Every time the electron-arm was hit we got a  $T3$  trigger, which set the third bit in the `DL.eventtypebits` variable to one. Because we are interested in all the events with a valid  $T3$  trigger we use logical masking to extract events with the third bit set to one.

- $|\delta_{Tg}| = \left| \frac{p - p_{central}}{p_{central}} \right| < 0.045$  : This cut corresponds to the momentum acceptance of the HRS-L spectrometer.
- $|\theta_{Tg}| < 0.06$  and  $|\theta_{Ph}| < 0.03$  : These two cuts represent the angular acceptance of the HRS-L spectrometer.

For each recorded event that passes the cuts I then determined  $\omega$  and  $Q^2$  and a product of the beam helicity and a target spin orientation:

$$h'_{target\&spin} = h_{beam} \times s_{target} = \begin{cases} (+) \times (+) = 1 \\ (+) \times (-) = -1 \\ (-) \times (+) = -1 \\ (-) \times (-) = 1 \end{cases} \quad (7)$$

For the calculation of the momentum transfer four-vector I used the standard functions that are included in our analysis software. Since our optics is not optimized yet the  $\omega$  and  $Q^2$  are not determined precisely, but they are good enough for our analysis. I have then divided the whole range in  $\omega \in [70, 250]$  into 18 equivalent regions and counted how many events with  $h' = 1$  and how many with  $h' = -1$  fall into each  $\omega$ -region. From there I was then able to calculate the raw experimental asymmetry for each region using the formula:

$$A_{exp}^i = \frac{\frac{N_i^+}{Q^+ f_d^+} - \frac{N_i^-}{Q^- f_d^-}}{\frac{N_i^+}{Q^+ f_d^+} + \frac{N_i^-}{Q^- f_d^-}}. \quad (8)$$

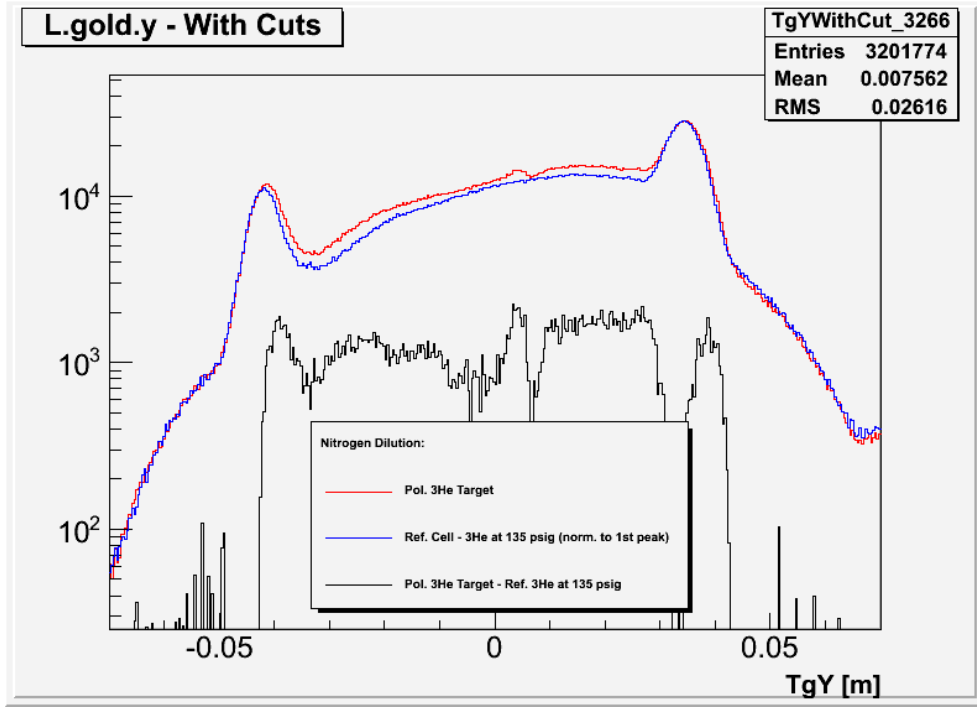


Figure 11: The red line represents the target  $y_{tg}$  coordinate for the production  ${}^3\text{He}$  runs, the blue line represents the  $y_{tg}$  coordinate for the reference-cell run with  $135\text{psig} = 150\text{psi} = 10.3\text{bar}$  of  ${}^3\text{He}$  and the black line represents the difference between the two.

Index  $i = 1\dots 18$  denotes a specific omega region and  $f_d^\pm$  is defined as

$$f_d^\pm = 1 + \frac{t_d^\pm}{t^\pm} \quad (9)$$

where  $t_d^\pm$  represents the dead time and  $t^\pm$  total measuring time with  $\pm$  beam helicity. It is not necessary that the same number of electrons in states  $h' = 1$  and  $h' = -1$  hits the target. We consider that by normalizing the number of counts with the collected charge  $Q^\pm$  in each state. Asymmetry must also be corrected for the dead time, which is also not necessarily the same for both states. However, looking at the run summary below we can see that the differences between the dead times and collected charges for both helicity states are very small and can be neglected in this analysis.

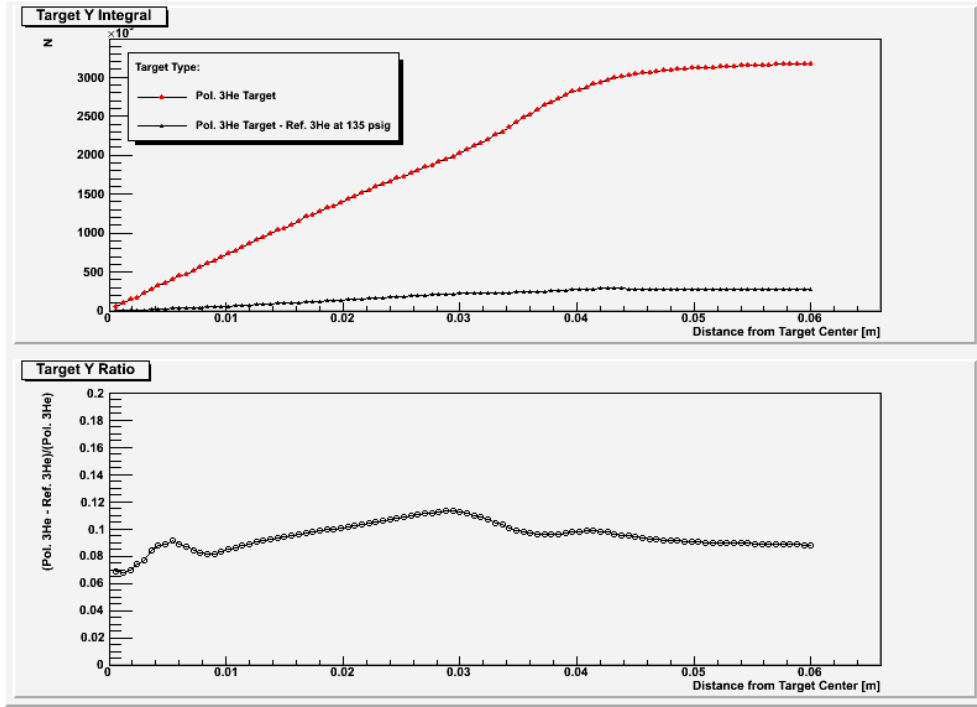


Figure 12: *Top*: Plot shows the integral of the Target  $y_{tg}$  histogram as a function of the distance from the target center. Red line corresponds to the full  ${}^3\text{He}$  run while the black line represents the integral of the nitrogen, that is contained in the production cell. *Bottom*: The ratio between the nitrogen yield ( ${}^3\text{He}^{Pol.} - {}^3\text{He}^{Ref.}(135psig)$ ) and a complete polarized target yield.

```

----- End-of-run Summary -----
PRESCALE FACTORS:ps1=16777215 ps2=16777215 ps3=5 ps4=4 ps5=1 ps6=1 ps7=65535 ps8=100

EVENTS : [ 0]: 4004671    [++]: 0          [--]: 1979590    [+]: 0          [-]: 1966956
TIME   : [ 0]: 33.010 mins [++]: 0.017 mins [--]: 16.290 mins [+]: 0.017 mins [-]: 16.298 mins

Test of Helicity gates
Time diff of helicity to nonhelicity times = 986.33221 seconds

LIVE calc. crudely accounts for correlations. Need offline calc.
DEAD TIME: [ 0]: 6.90%    [++]: 0.00%    [--]: 6.88%    [+]: 0.00%    [-]: 6.84%

APPROXIMATE BCM CHARGES (C)
BCM u1 [ 0]:0.0174      BCM u3 [ 0]:0.01739      BCM u10 [ 0]:0.01539
BCM u1 [++]:0          BCM u3 [++]:0          BCM u10 [++]:0
BCM u1 [--]:0.008575   BCM u3 [--]:0.008566   BCM u10 [--]:0.00758
BCM u1 [+]:0          BCM u3 [+]:0          BCM u10 [+]:0
BCM u1 [-]:0.008571   BCM u3 [-]:0.008566   BCM u10 [-]:0.00758

```

Our final formula for the calculation of the Asymmetry is then:

$$A_{exp}^i = \frac{N_i^+ - N_i^-}{N_i^+ + N_i^-}. \quad (10)$$

Now we need to consider that the measured asymmetries are smaller than the true physical asymmetries because the target and beam are not 100% polarized and because of the nitrogen dilution. The physical asymmetry can be calculated as:

$$A_{physical}^i = \frac{A_{exp}^i}{P_{target}P_{beam}} \times f_{nitrogen} \quad (11)$$

We would also like to determine the error of this asymmetry. It can be written as:

$$\Delta A_{exp} = \frac{1 - A_{exp}}{\sqrt{N^+ + N^-}} \approx \frac{1}{\sqrt{N}}, \quad (12)$$

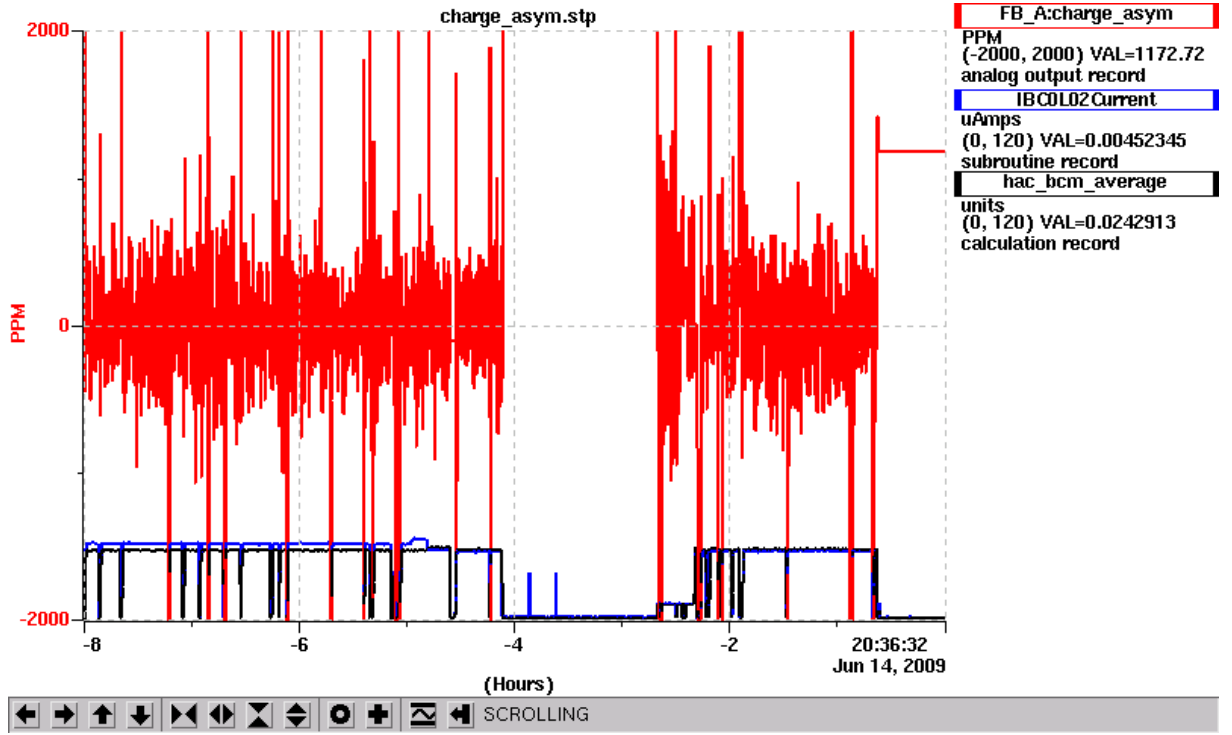


Figure 13: Plot shows the readout values from the Happex system, that measured the beam charge asymmetry at different times during the experiment.

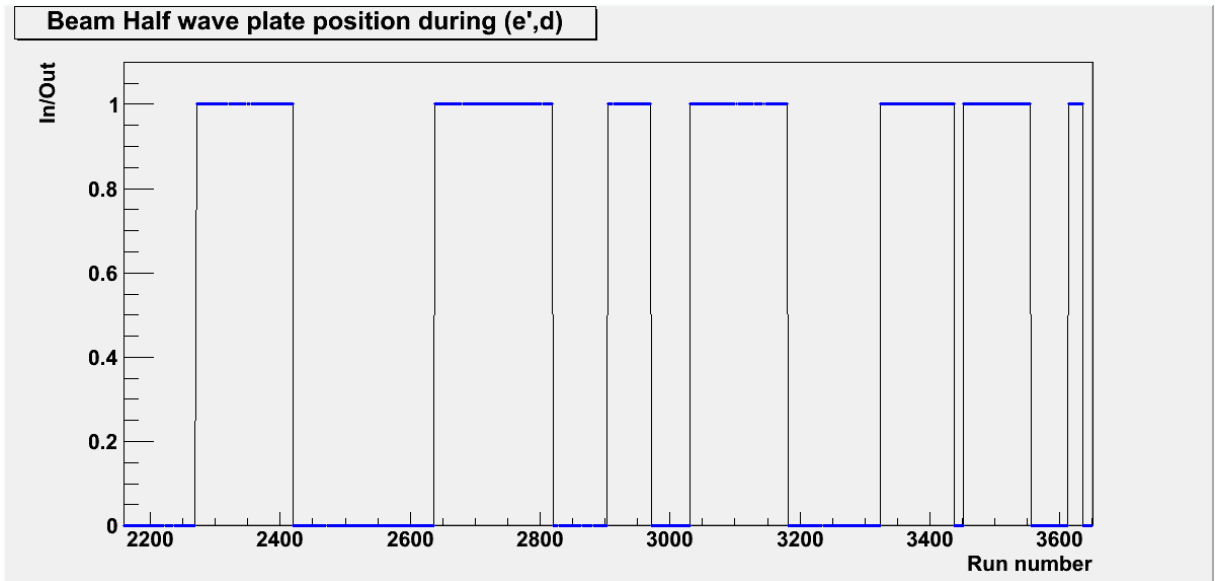


Figure 14: Position (IN or OUT) of the beam half-wave-plate during the experiment.

where we assume that the asymmetries that we measure are small and consequently:

$$\Delta A_{physical} = \frac{\Delta A_{exp}}{P_{target} P_{beam}} \times f_{nitrogen} \quad (13)$$

In this analysis I have analyzed approximately 200 runs. For each run I have calculated the asymmetries for all  $\omega$ -regions. When all the data were analyzed I calculated the mean asymmetry and the error of the these

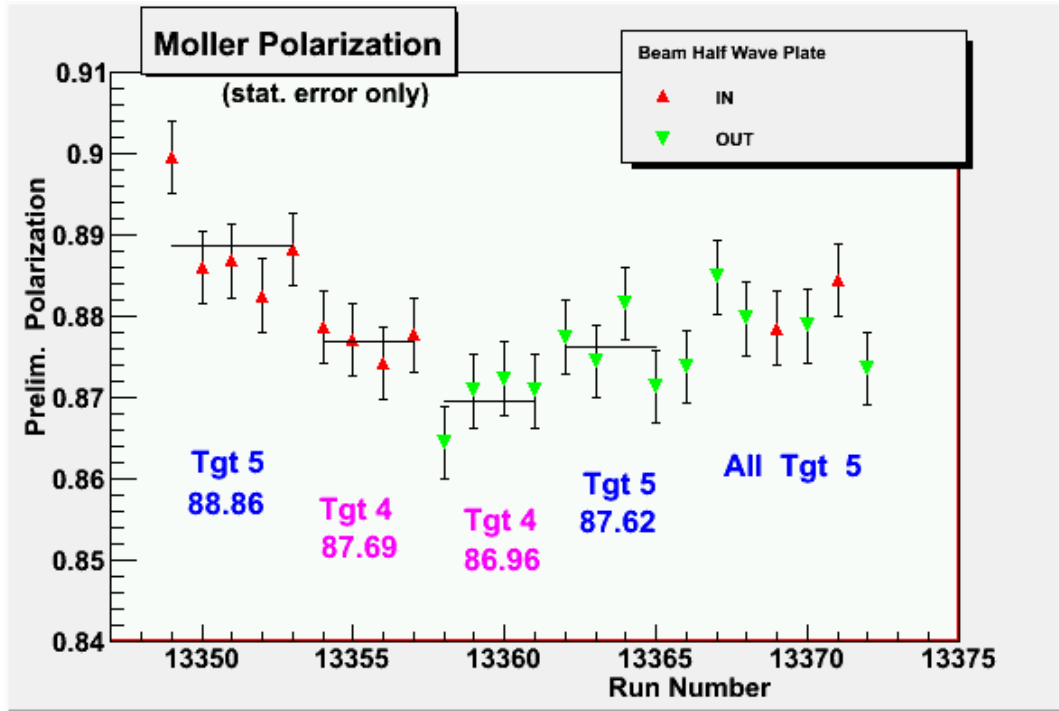


Figure 15: An example of a Møller measurement results.

asymmetries. I have done this analysis for three sets of data. First two sets were both  $Q^2 \approx 0.3(\text{GeV}/c)^2$  data from the HRS-L spectrometer but one set was measured with the beam half-wave plate IN while the other was measured with the half-wave plate OUT. As mentioned before it is useful to check if the asymmetries flip when the position of the HWP is changed. The third set contained the  $Q^2 \approx 0.4(\text{GeV}/c)^2$  data measured with the HRS-R.

My results are shown in figures 16 to 21. I have compared my results with the  $G_M^n$  asymmetries and the results agree surprisingly well. I should stress that these results should not be taken too seriously at the moment because this is only a quick estimate. However, the thing that we can learn from these results is that the asymmetries do change when the HWP state is changed and that they have the correct sign and follow the correct trend. This gives us more faith in our data.

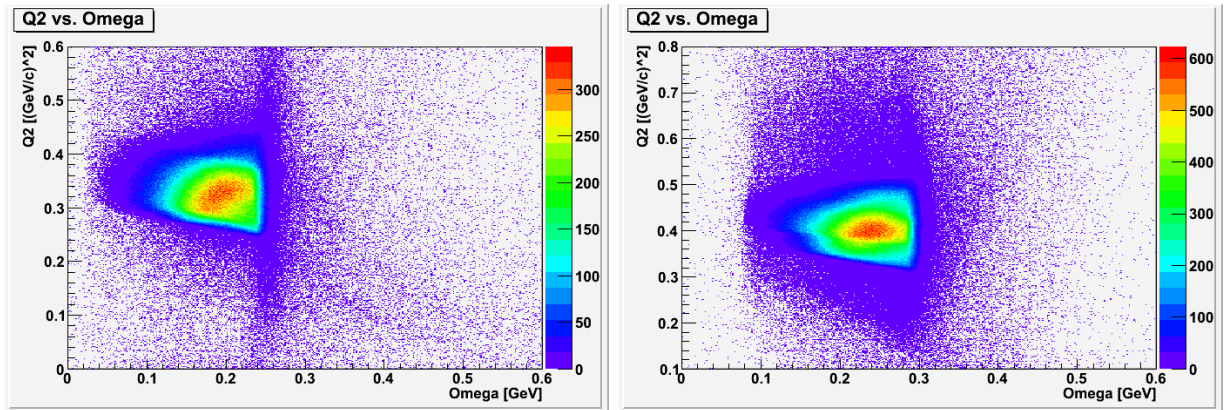


Figure 16: *Left*:  $\omega$  vs.  $Q^2$  plot for the  $Q^2 = 0.3(\text{GeV}/c)^2$  data. *Right*:  $\omega$  vs.  $Q^2$  plot for the  $Q^2 = 0.4(\text{GeV}/c)^2$  data.

## References

- [1] F. Halzen A. D. Martin, *Quarks and Leptons*, An Introductory Course in Modern particle Physics, John Wiley & Sons. Inc.
- [2] W. Xu et al., *Phys. Rev. Lett.* **85**, 2900 (2000)
- [3] *Measurement of  $A_x$  and  $A_z$  asymmetries in the quasi-elastic  ${}^3\vec{H}e(\vec{e}, e'd)$  reaction*, Hall A Proposal to JLab PAC 22 for the Experiment E05-102, W. Bertozzi, Z.-L Zhou, D. W. Higinbotham, S. Širca, B. E. Norum (co-spokespersons), May 27, 2002

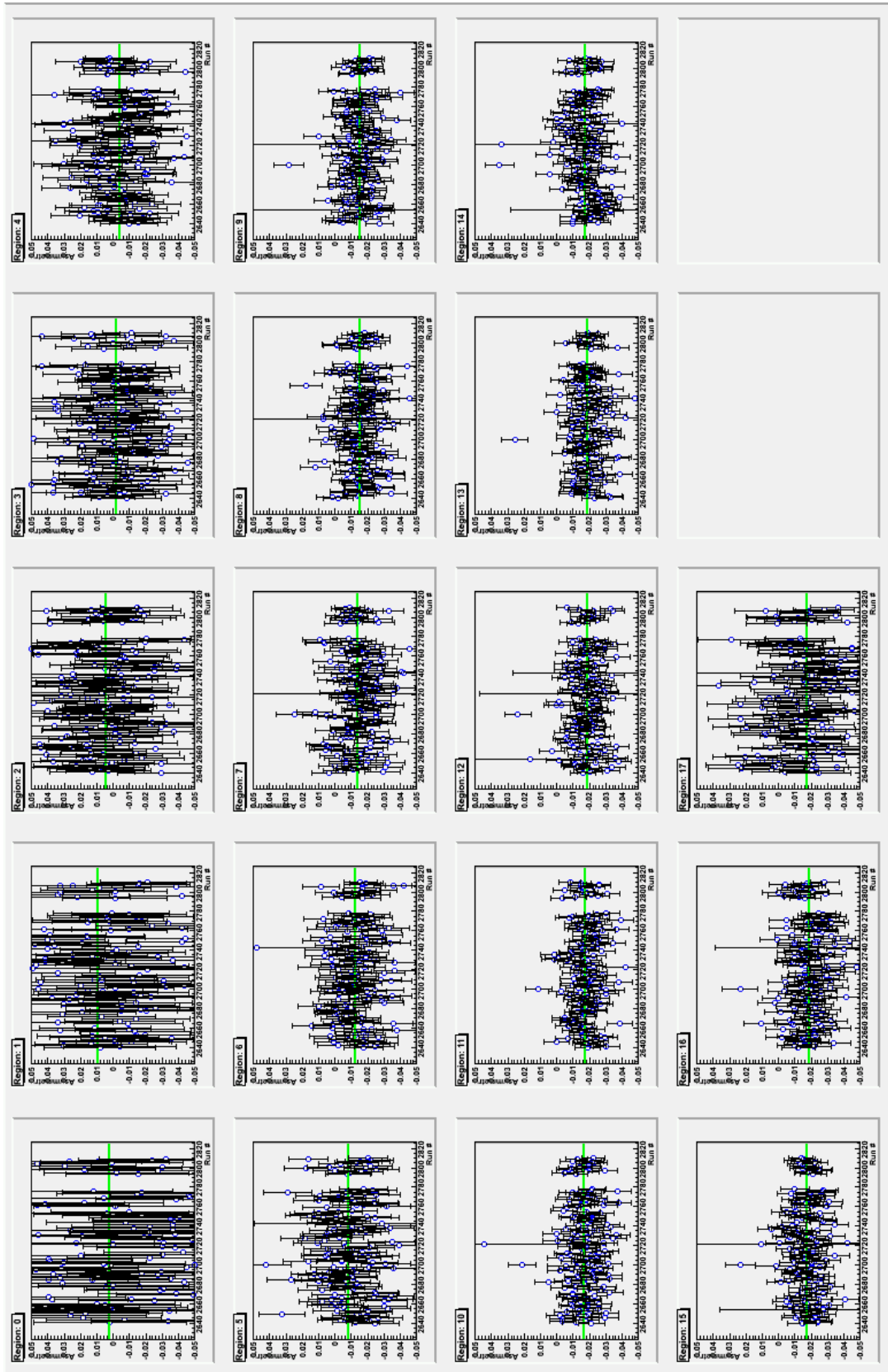


Figure 17: The calculated asymmetries  $A_t$  inside each  $\omega$ -region for all  $Q^2 = 0.3(\text{GeV}/c)^2$  data with HWP-In. The central values of each region are :  $\omega = 80.0, 90.0, 100.0, 110.0, 120.0, 130.0, 140.0, 150.0, 160.0, 170.0, 180.0, 190.0, 200.0, 210.0, 220.0, 230.0, 240.0, 250.0$  MeV.

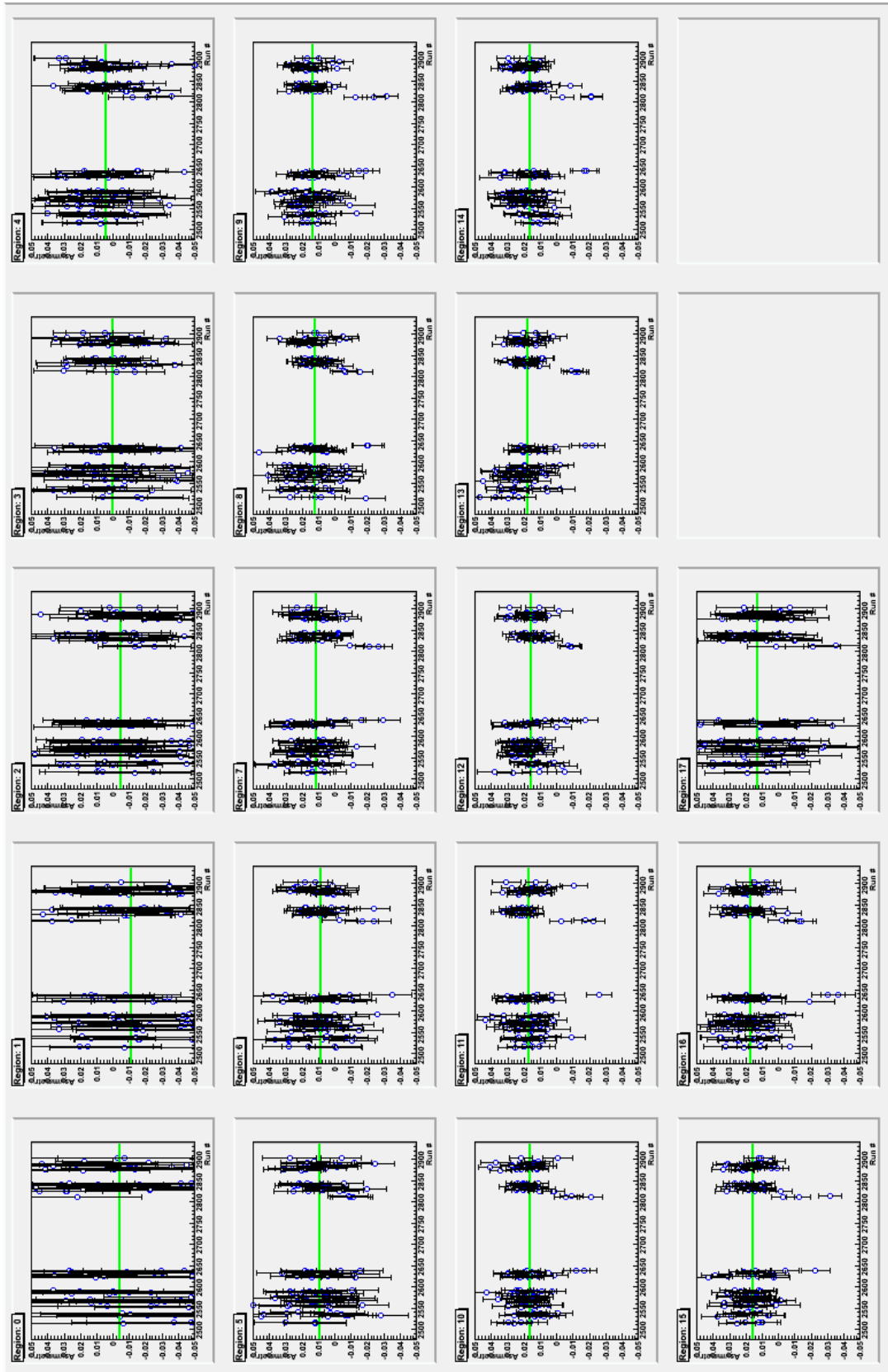


Figure 18: The calculated asymmetries  $A_{t'}$  inside each  $\omega$ -region for all  $Q^2 = 0.3(\text{GeV}/c)^2$  data with HWP-Out. The central values of each region are :  $\omega = 80.0, 90.0, 100.0, 110.0, 120.0, 130.0, 140.0, 150.0, 160.0, 170.0, 180.0, 190.0, 200.0, 210.0, 220.0, 230.0, 240.0, 250.0$  MeV.



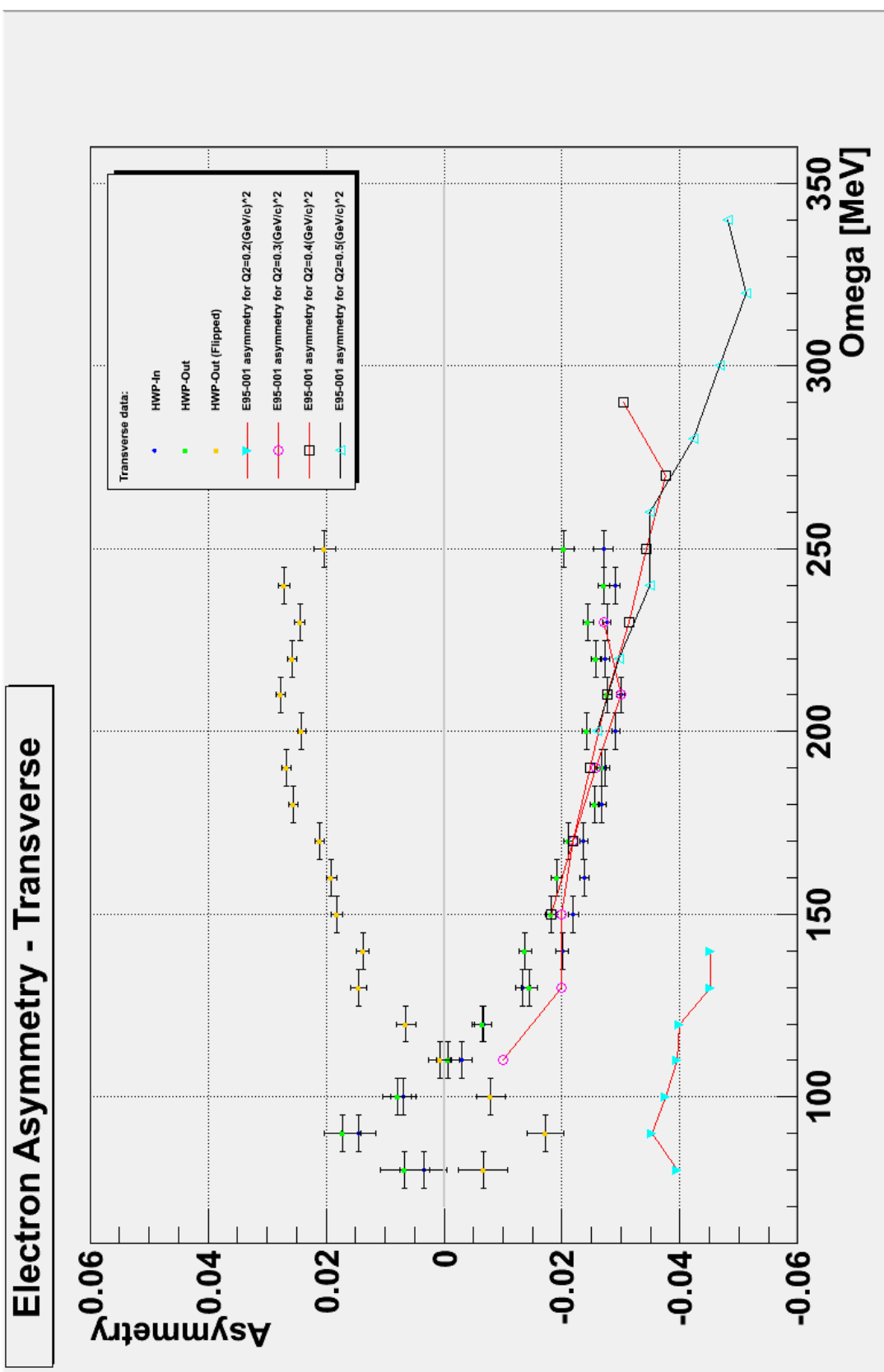


Figure 19: The calculated asymmetries  $A_t^n$  for the  $Q^2 = 0.3(\text{GeV}/c)^2$  data as a function of  $\omega$ . I compared my results with the  $G_M^n$  asymmetries at different  $Q^2$ . Since I did not perform any cuts on  $Q^2$  my  $Q^2$  region is much broader. Therefore my asymmetries are probably weighted combination of  $G_M^n$ 's  $Q^2 = 0.3(\text{GeV}/c)^2$  and  $Q^2 = 0.4(\text{GeV}/c)^2$  asymmetries.

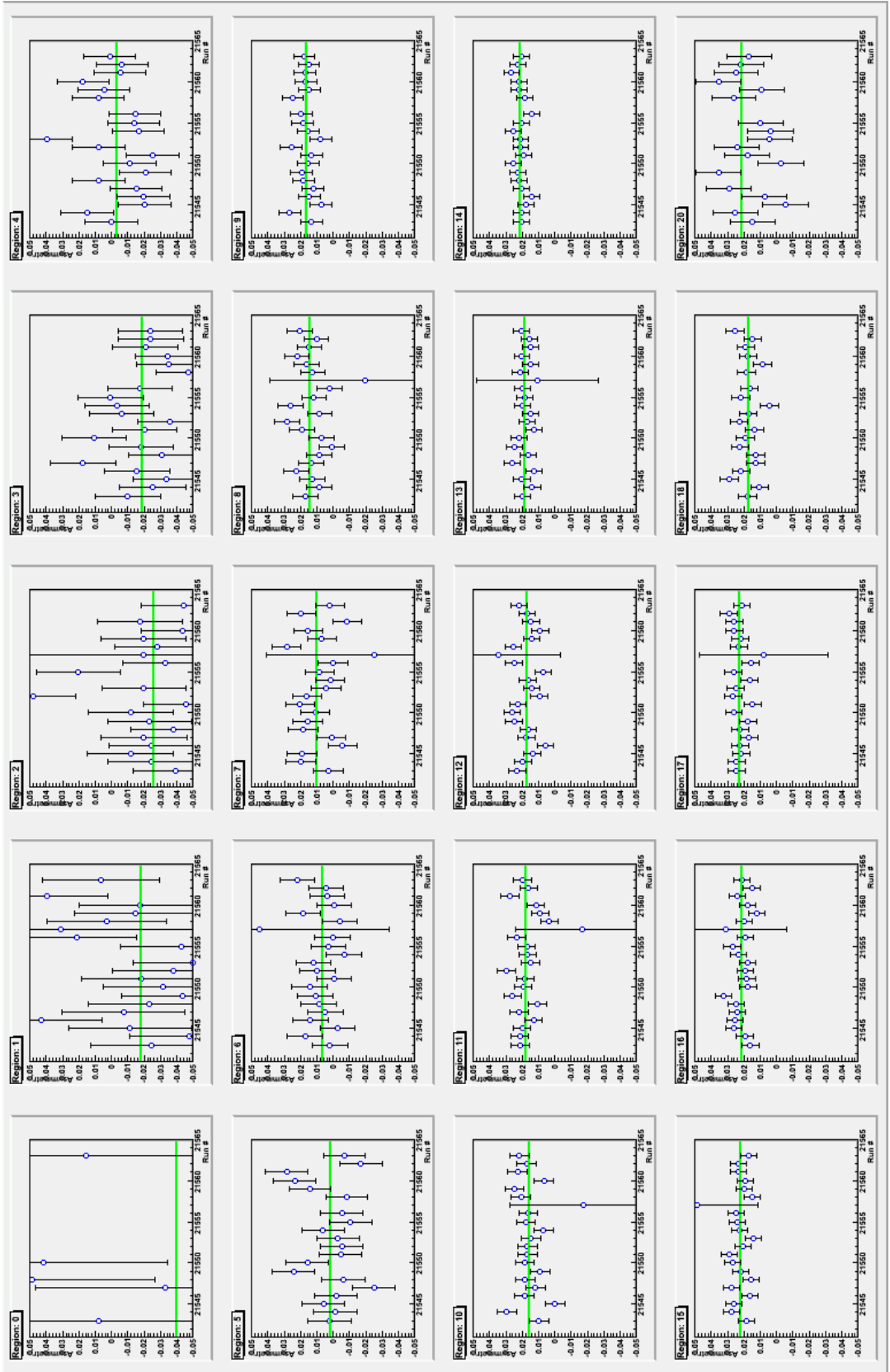


Figure 20: The calculated asymmetries  $A_{\nu}$  inside each  $\omega$ -region for all  $Q^2 = 0.4(\text{GeV}/c)^2$  data with HWP-Out. The central values of each region are :  $\omega = 100.0, 110.0, 120.0, 130.0, 140.0, 150.0, 160.0, 170.0, 180.0, 190.0, 200.0, 210.0, 220.0, 230.0, 240.0, 250.0, 260.0, 270.0, 280.0, 290.0, 300.0$  MeV.

## HRS-R Electron Asymmetry - Transverse

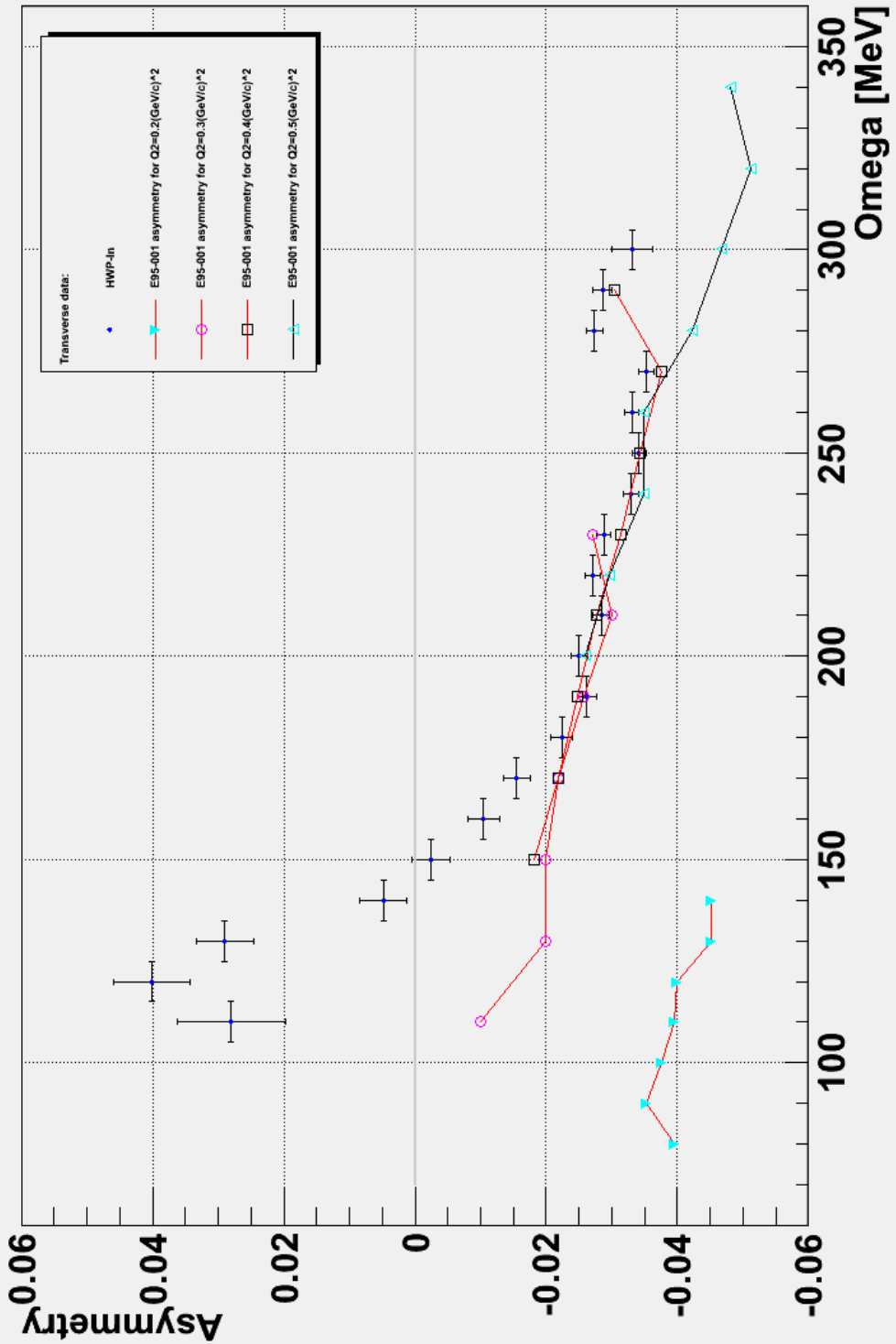


Figure 21: The calculated asymmetries  $A_t^{\nu}$  for the  $Q^2 = 0.4(\text{GeV}/c)^2$  data as a function of  $\omega$ . I compared my results with the  $G_M^n$  asymmetries at different  $Q^2$ . Since I did not perform any cuts on  $Q^2$  my  $Q^2$  region is much broader. Therefore my asymmetries are probably weighted combination of  $G_M^n$ 's  $Q^2 = 0.4(\text{GeV}/c)^2$  and  $Q^2 = 0.5(\text{GeV}/c)^2$  asymmetries.